Supporting information for:

Spiroplasma shows a *Wolbachia*-like effect in hampering virus replication in spider mite

Lucas Yago Melo Ferreira[1], João Pedro Nunes Santos[1], David Gabriel do Nascimento Souza[1], Lixsy Celeste Bernardez Orellana[1], Sabrina Ferreira de Santana[1], Anderson Gonçalves Sousa[1], Paula Luize Camargos Fonseca[2], Amanda Gabrielly Santana Silva[1], Vinicius Castro Santos[2], Isaque João da Silva de Faria[3], Roenick Proveti Olmo[4], Luis Gustavo Carvalho Pacheco[5], Marcio Gilberto Cardoso Costa[1], Carlos Priminho Pirovani[1], Anibal Ramadan Oliveira[6], Eric Roberto Guimarães Rocha Aguiar[1*]

[1]Center of Biotechnology and Genetics, Department of Biological Sciences, Universidade Estadual de Santa Cruz, Rodovia Jorge Amado, km 16, Ilhéus, Bahia, Brazil, 45662-900.

[2]Institute of Biological Sciences, Department of Microbiology, Universidade Federal de Minas Gerais, Belo Horizonte 31270-901, Brazil.

[3]Department of Biochemistry and Immunology, Instituto de Ciencias Biológicas, Universidade Federal de Minas Gerais, Belo Horizonte, Minas Gerais, CEP 30270–901, Brazil

[4]CNRS-UPR9022, Institut de Biologie Moléculaire et Cellulaire, 67084 Strasbourg Cedex, France

[5]Department of Biotechnology, Institute of Health Sciences, Universidade Federal da Bahia (UFBA). Av. Reitor Miguel Calmon, s/n, Vale do Canela, Salvador-Bahia, 40.110-100, Brazil.

[6] Laboratory of Entomology, Department of Biological Science, Universidade Estadual de Santa Cruz, Rodovia Jorge Amado, km 16, Ilhéus, Bahia, Brazil, 45662-900.

*Aguiar E.R.G.R

Email: ericgdp@gmail.com

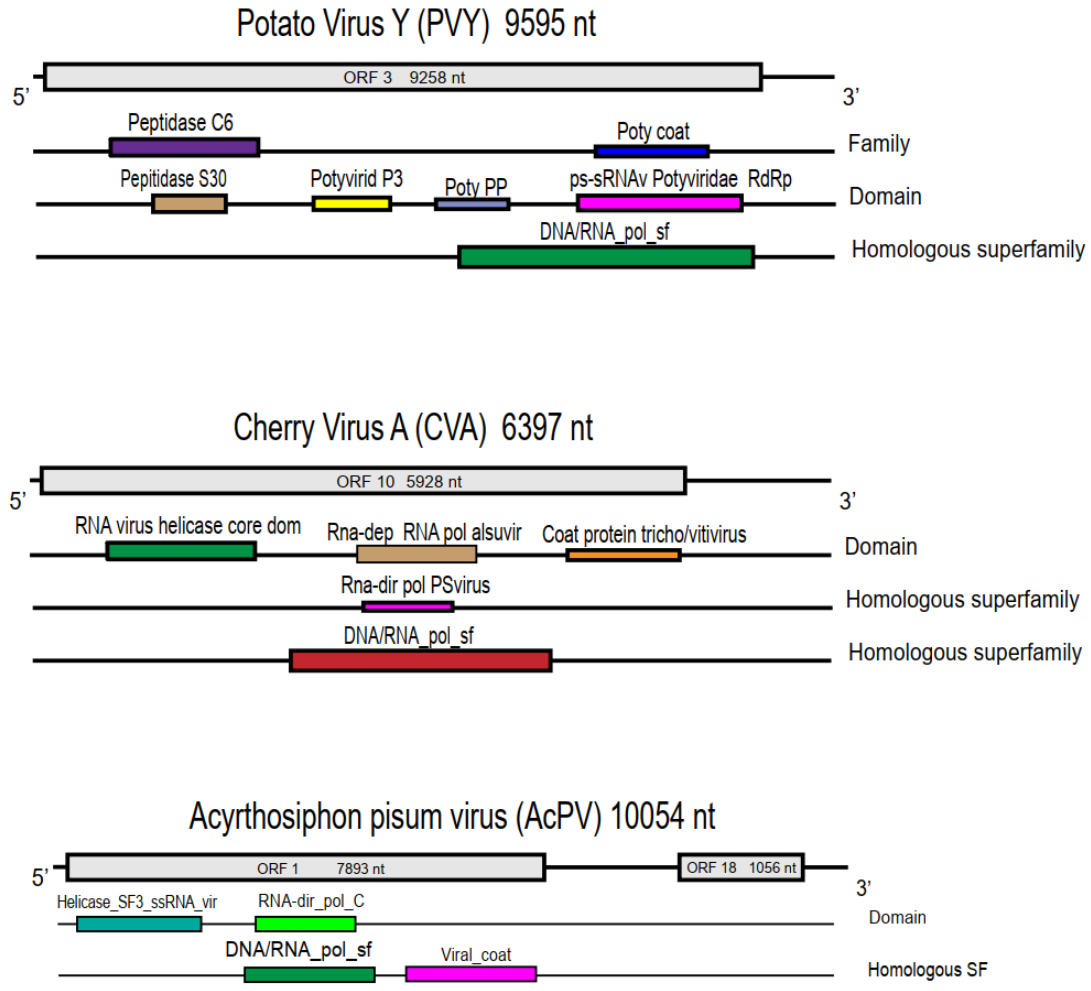

Figure S1. Genome characteristics and conserved structures of the *Potato Virus Y*, *Cherry virus A* and *Acyrthosiphon pisum virus* viral sequences characterized in *Tetranychus truncatus*. The ORFfinder program was used to identify the largest ORF and InterProScan program was used to identify conserved structures.

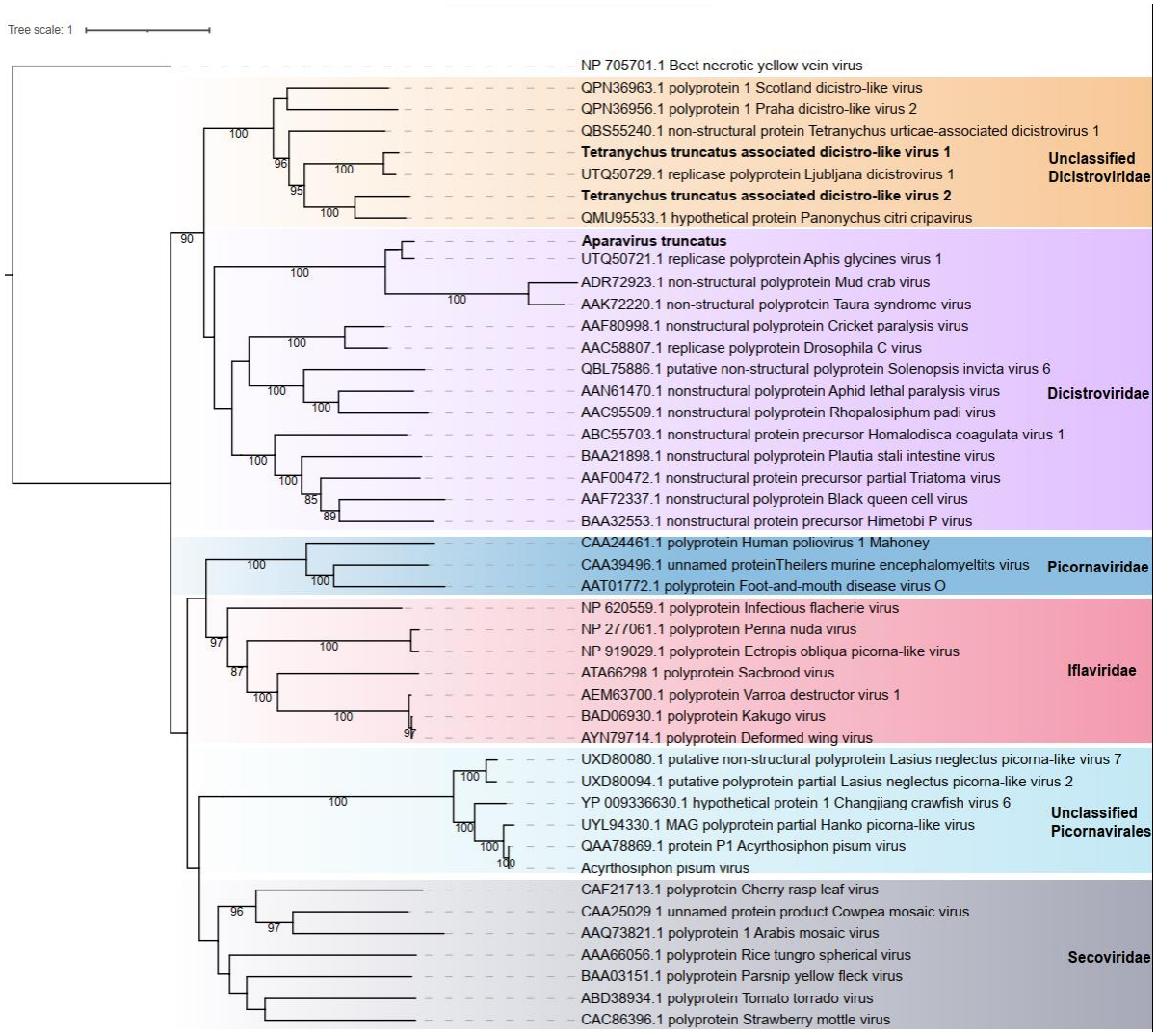

Figure S2. Characterization of the novel TtDV-1, TtDV-2 and AVT viruses. Phylogenetic analysis, conducted using ModelTest-NG based on the Akaike information criterion (AIC), determined VT+F as the optimal evolutionary model. Bootstrap values were generated from 1000 replicates. Values below 70% are not displayed.

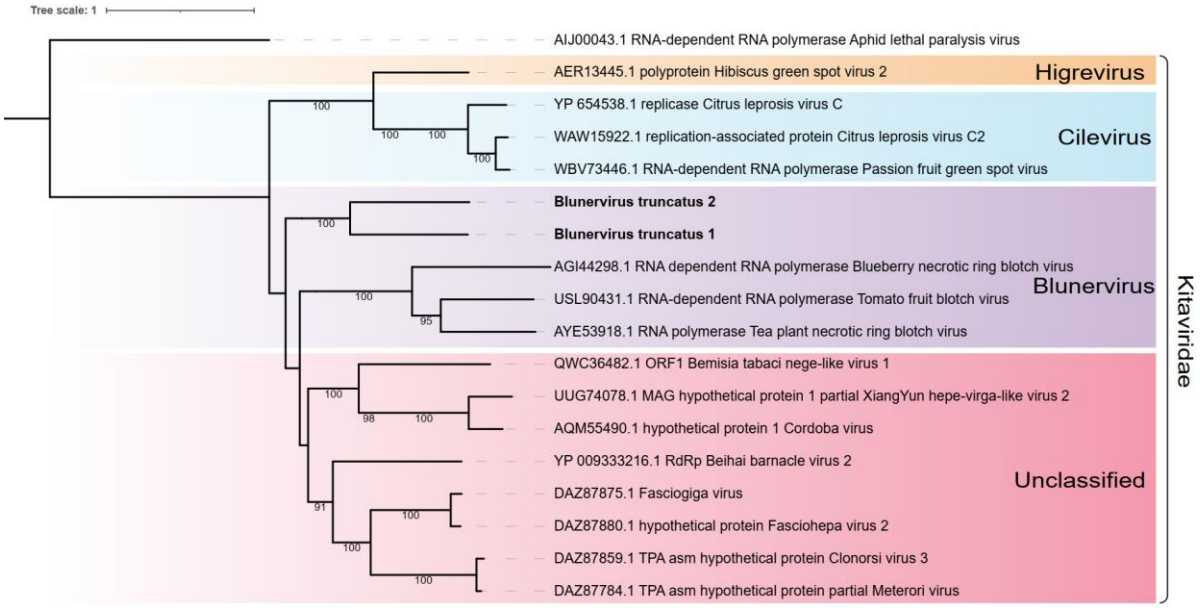

Figure S3. Characterization of the novel BVT-1 and BVT-2 viruses. Phylogenetic analysis, conducted using ModelTest-NG based on the Akaike information criterion (AIC), determined VT+F as the optimal evolutionary model. Bootstrap values were generated from 1000 replicates. Values below 70% are not displayed.

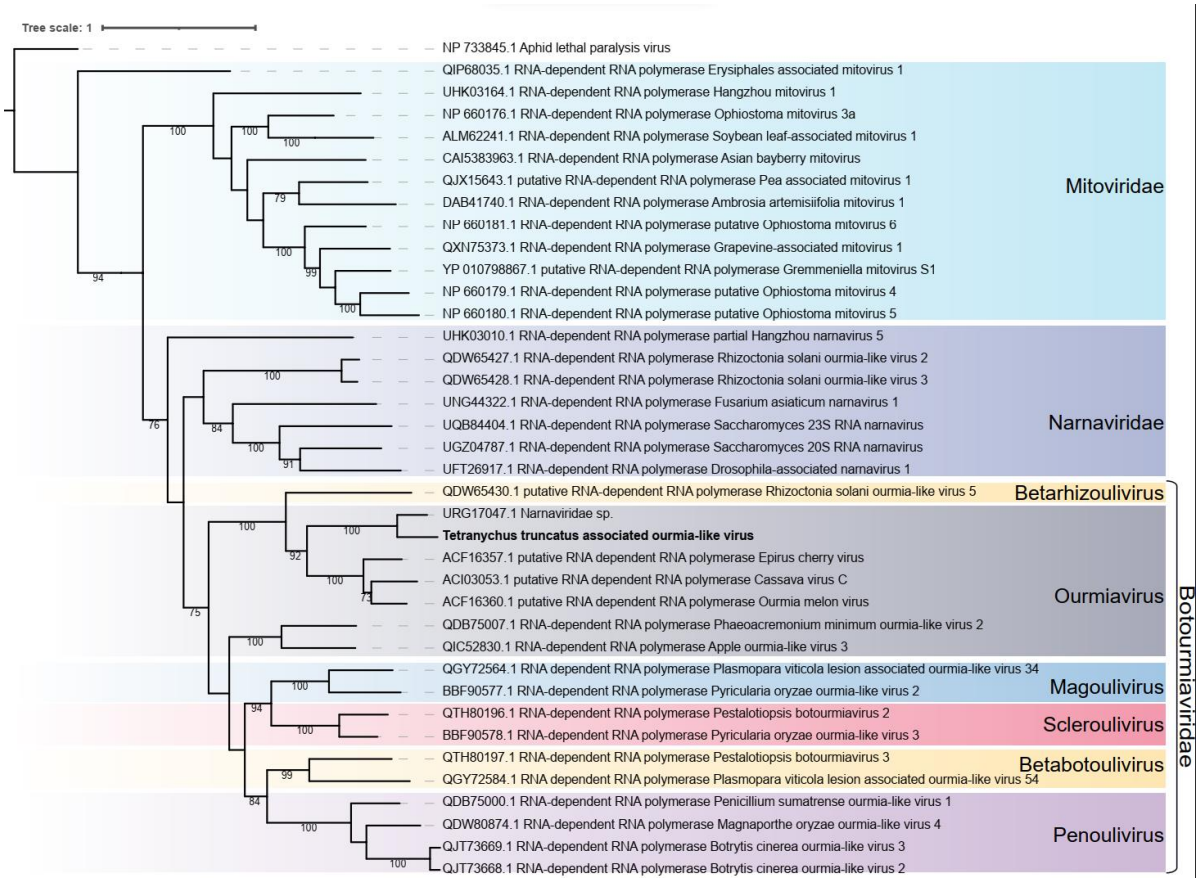

Figure S4. Characterization of the novel TtOV virus. Phylogenetic analysis, conducted using ModelTest-NG based on the Akaike information criterion (AIC), determined VT+F as the optimal evolutionary model. Bootstrap values were generated from 1000 replicates. Values below 70% are not displayed.

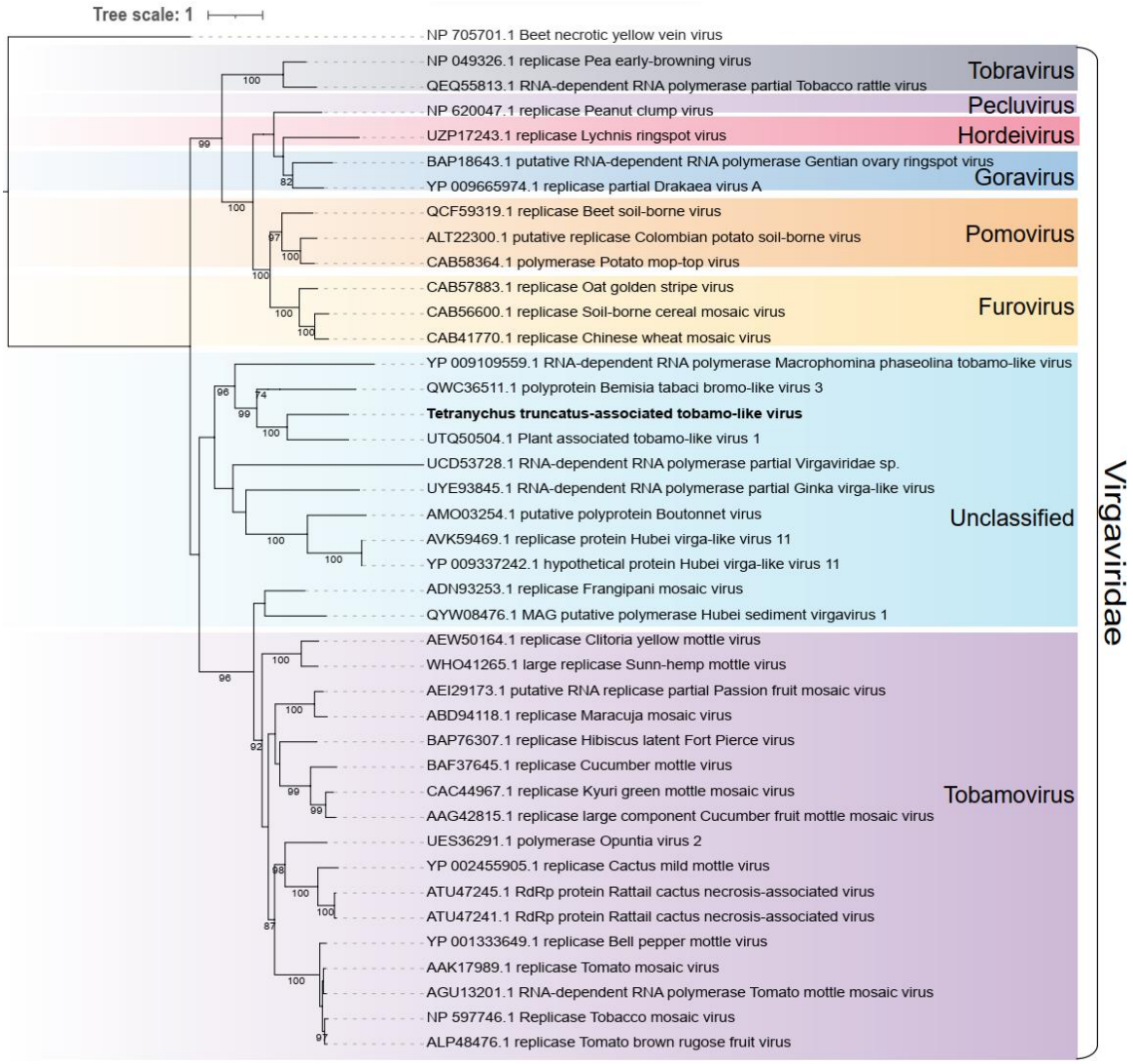

Figure S5. Characterization of the novel TtTV virus. Phylogenetic analysis, conducted using ModelTest-NG based on the Akaike information criterion (AIC), determined VT+F as the optimal evolutionary model. Bootstrap values were generated from 1000 replicates. Values below 70% are not displayed.

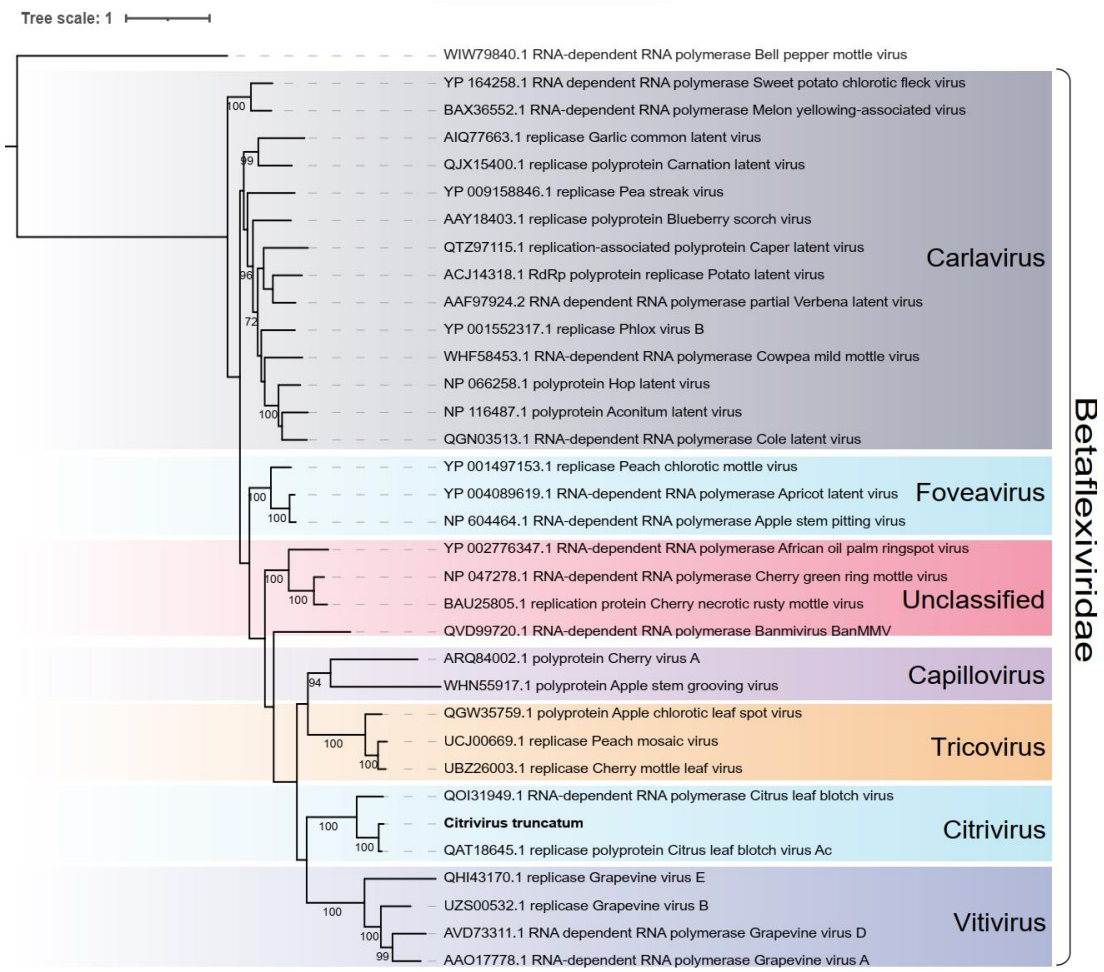

Figure S6. Characterization of the novel CVT virus. Phylogenetic analysis, conducted using ModelTest-NG based on the Akaike information criterion (AIC), determined VT+F as the optimal evolutionary model. Bootstrap values were generated from 1000 replicates. Values below 70% are not displayed.

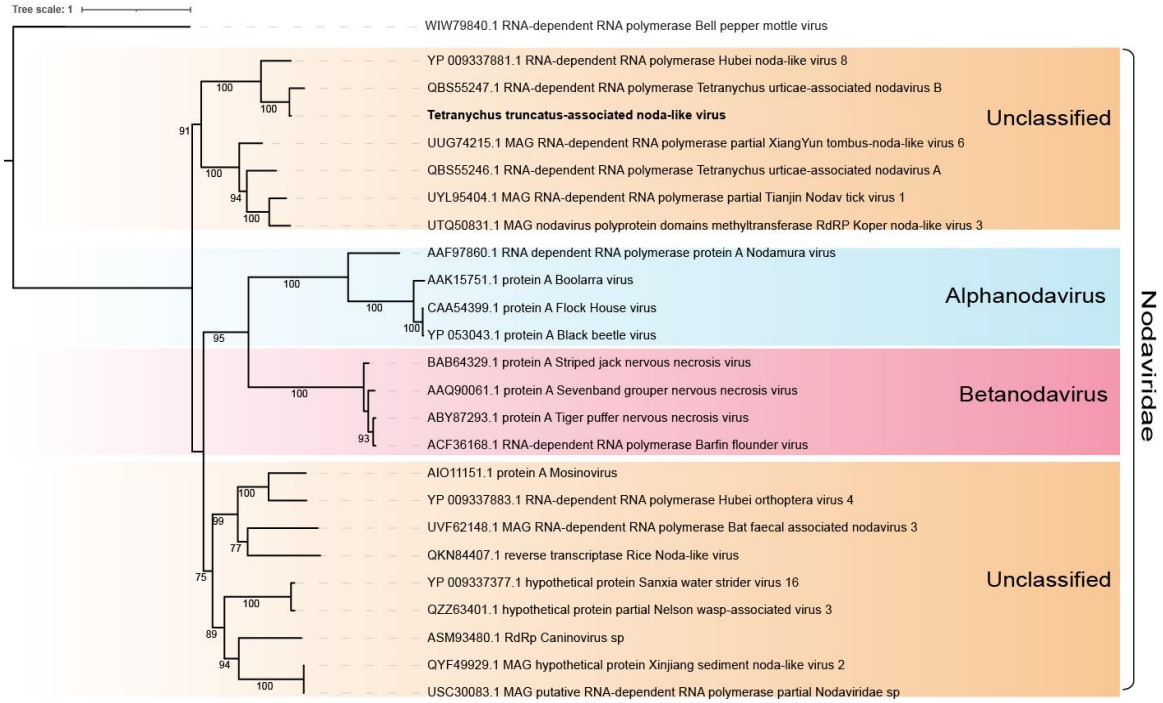

Figure S7. Characterization of the novel TtNoV virus. Phylogenetic analysis, conducted using ModelTest-NG based on the Akaike information criterion (AIC), determined VT+F as the optimal evolutionary model. Bootstrap values were generated from 1000 replicates. Values below 70% are not displayed.

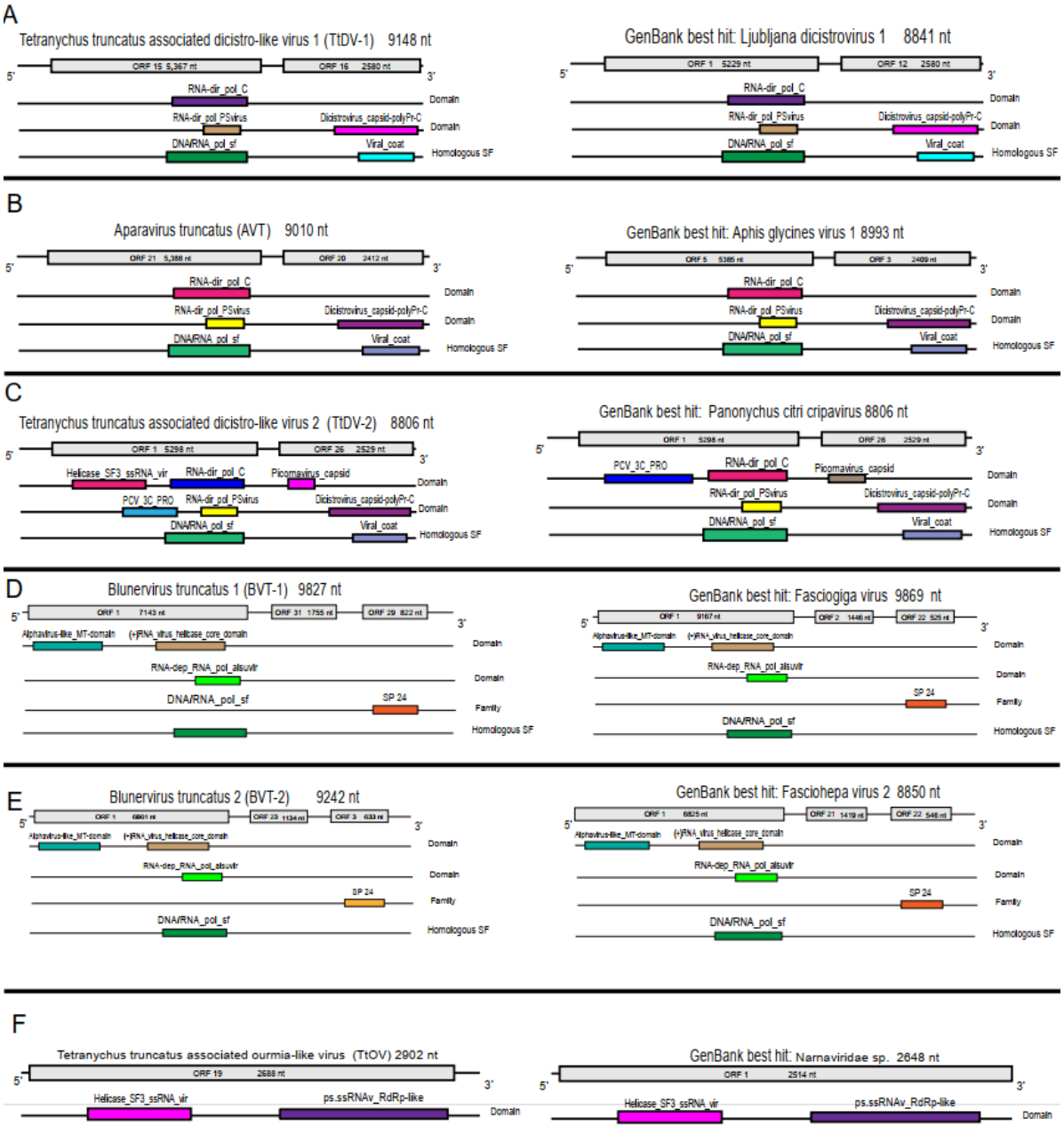

Figure S8. Genome characteristics and conserved structures of the characterized viral sequences related to Dicistroviruses, Kitaviruses, and Ourmiavirus and their best hits. The structural annotation of the characterized viruses associated with *Tetranychus truncatus* is depicted on the left, while their GenBank best hits are shown on the right. The ORFfinder program was used to identify the largest open reading frames (ORFs), and the InterProScan program was employed to identify conserved structures within these viral sequences.

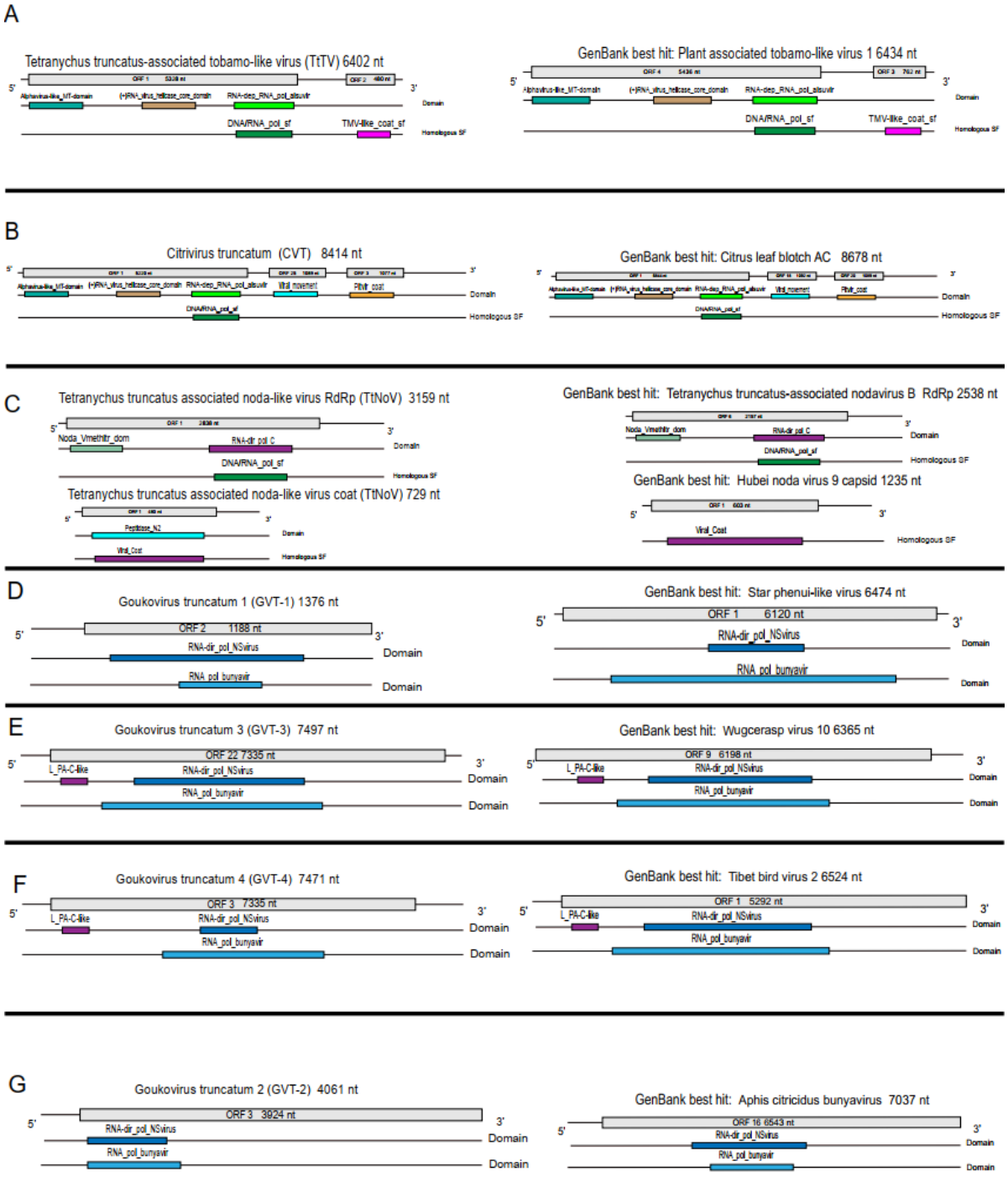

Figure S9. Genome characteristics and conserved structures of the characterized viral sequences related to Tobamoviruses, Citriviruses, Nodaviruses, and Phenuiviruses and their best hits. The structural annotation of the characterized viruses associated with *Tetranychus truncatus* is depicted on the left, while their GenBank best hits are shown on the right. The ORFfinder program was used to identify the largest open reading frames (ORFs), and the InterProScan program was employed to identify conserved structures within these viral sequences.

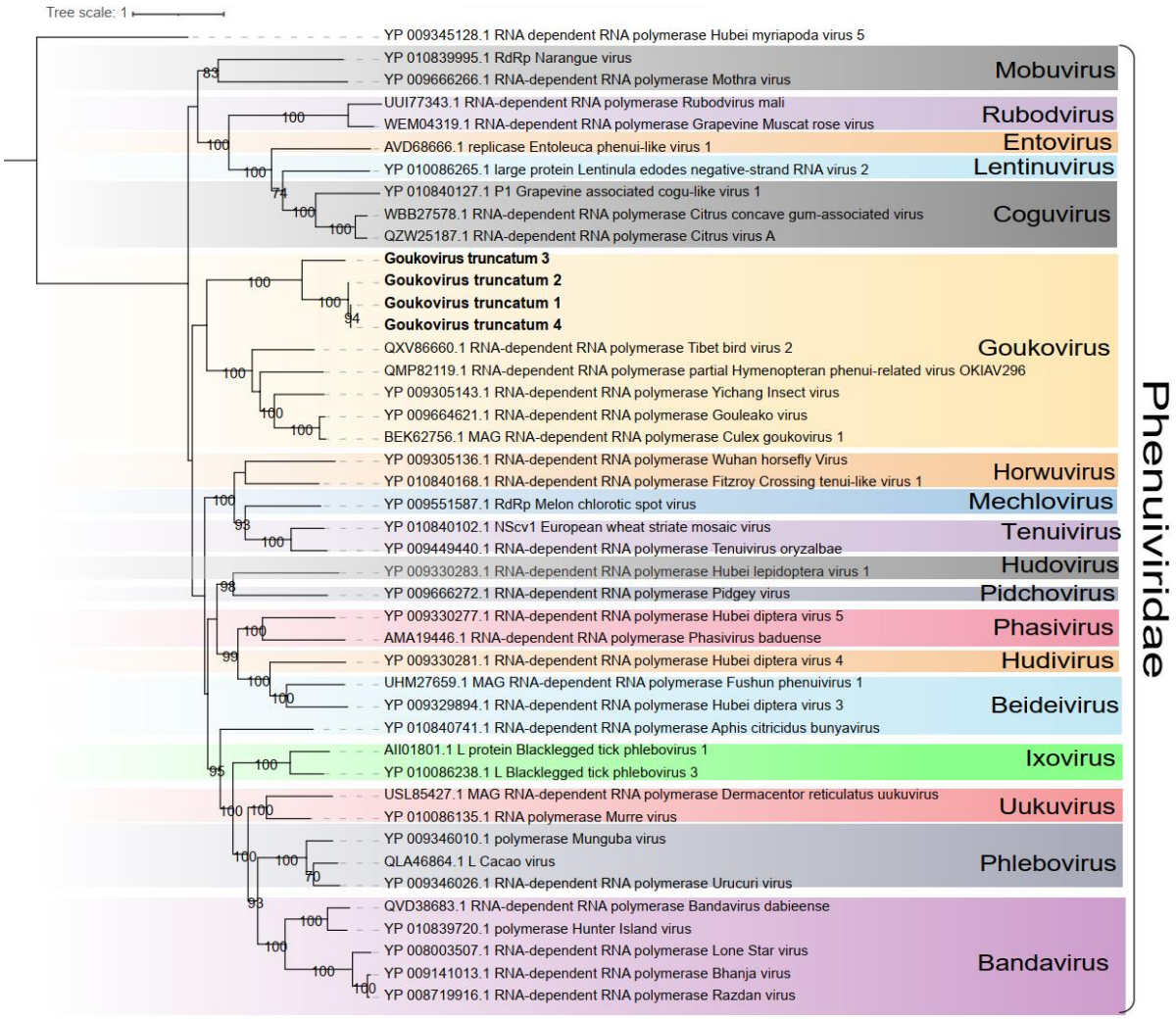

Figure S10. Characterization of the novel GVT-1, GVT-2, GVT-3 and GVT-4 viruses. Phylogenetic analysis, conducted using ModelTest-NG based on the Akaike information criterion (AIC), determined VT+F as the optimal evolutionary model. Bootstrap values were generated from 1000 replicates. Values below 70% are not displayed.

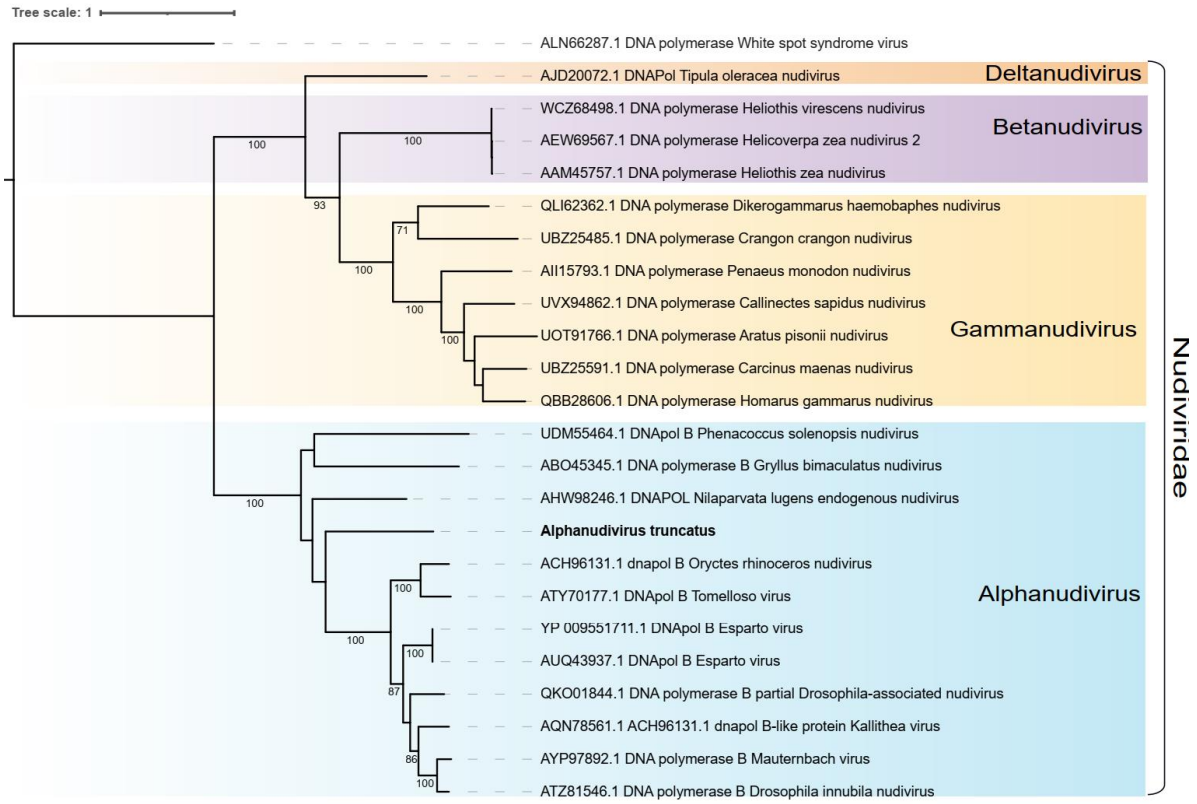

Figure S11. Characterization of the novel GVT-1, GVT-2, GVT-3 and GVT-4 viruses. Phylogenetic analysis, conducted using ModelTest-NG based on the Akaike information criterion (AIC), determined VT+F as the optimal evolutionary model. Bootstrap values were generated from 1000 replicates. Values below 70% are not displayed.

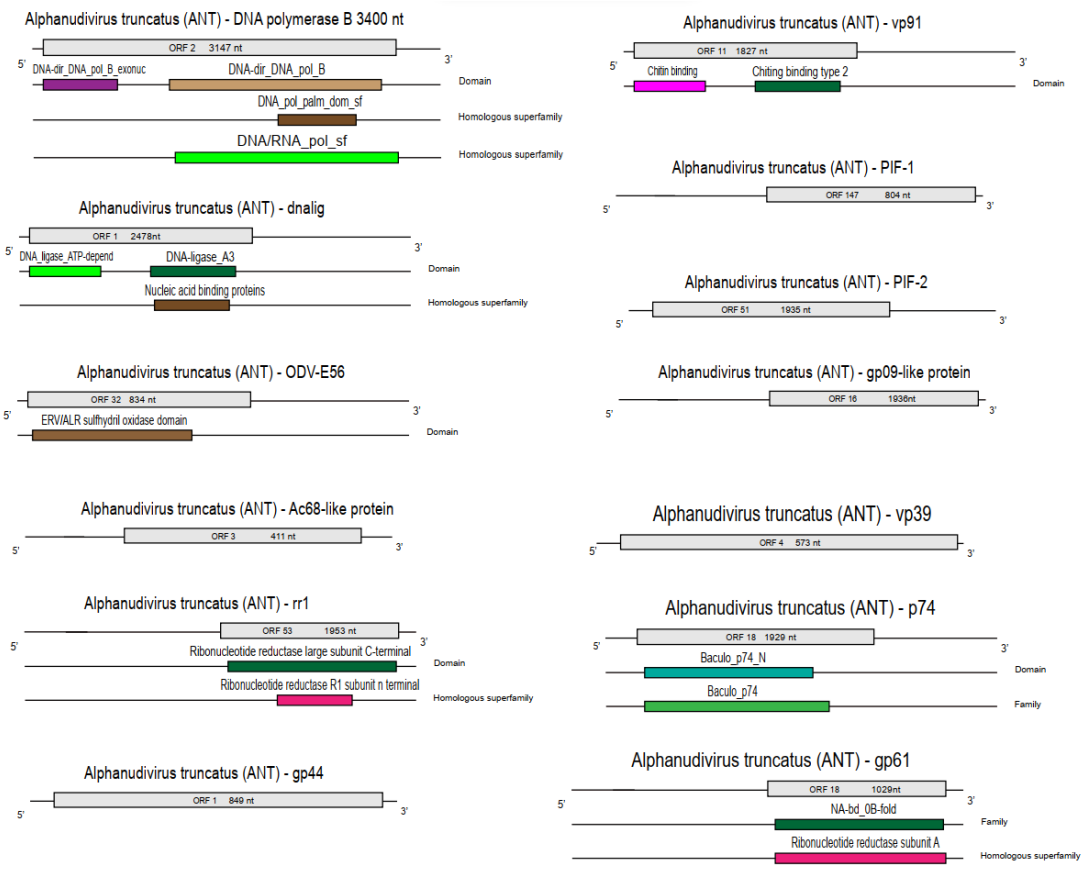

Figure S12. Genome characteristics and conserved structures of the *Alphanudivirus truncatus* core genes sequences. The ORFfinder program was used to identify the largest ORF and InterProScan program was used to identify conserved structures.

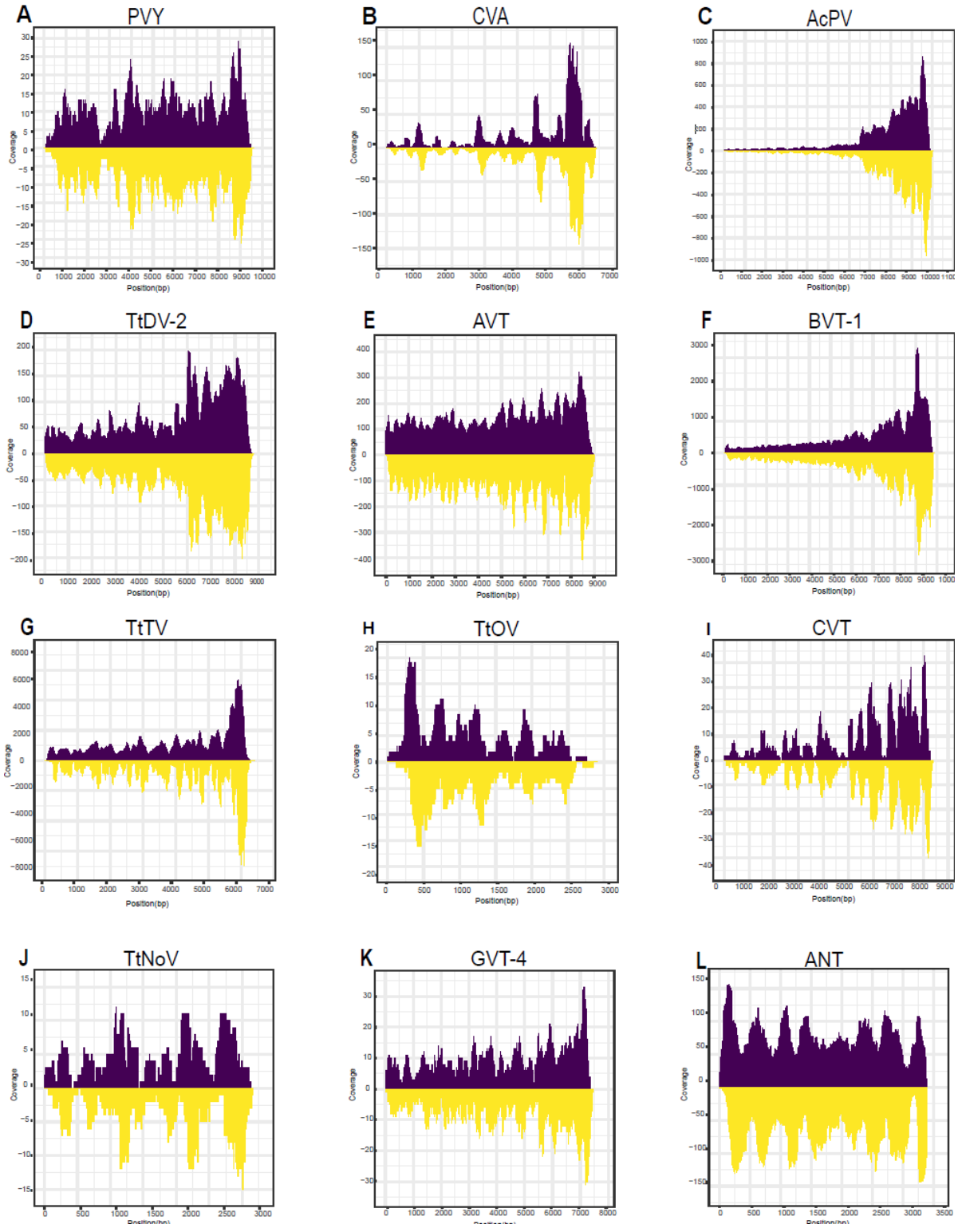

Figure S13. **RNA density coverage plots of known and novel viral sequences**. RNA density plots illustrating the coverage profiles of both known viruses (A-C) and newly characterized viruses (D – L), with RNA sense depicted in blue and antisense in yellow. The Y-axis denotes the total coverage, while the X-axis indicates the position of the base pair along the sequence's total length.

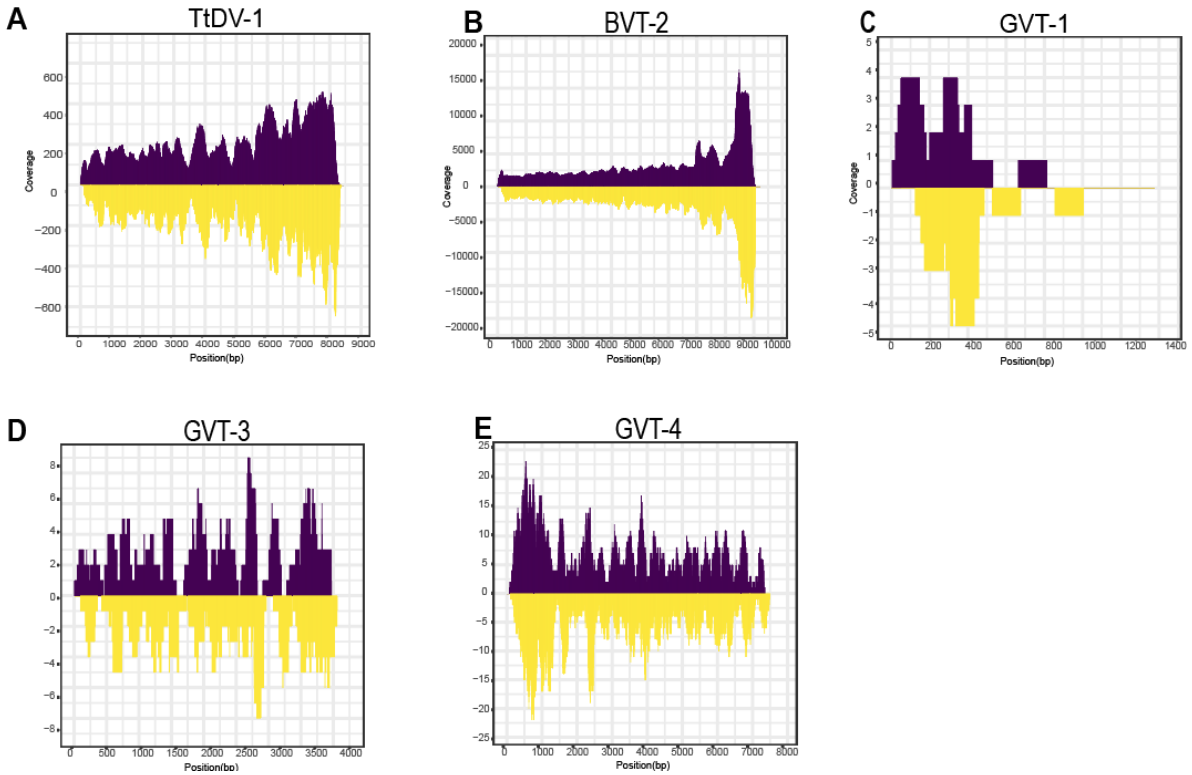

Figure S14: **RNA density coverage plots of characterized viral sequences**. RNA density plots illustrate the coverage profiles of newly characterized viruses (A-E), with RNA sense depicted in blue and antisense in yellow. The Y-axis denotes the total coverage, while the X-axis indicates the position of the base pair along the sequence's total length.

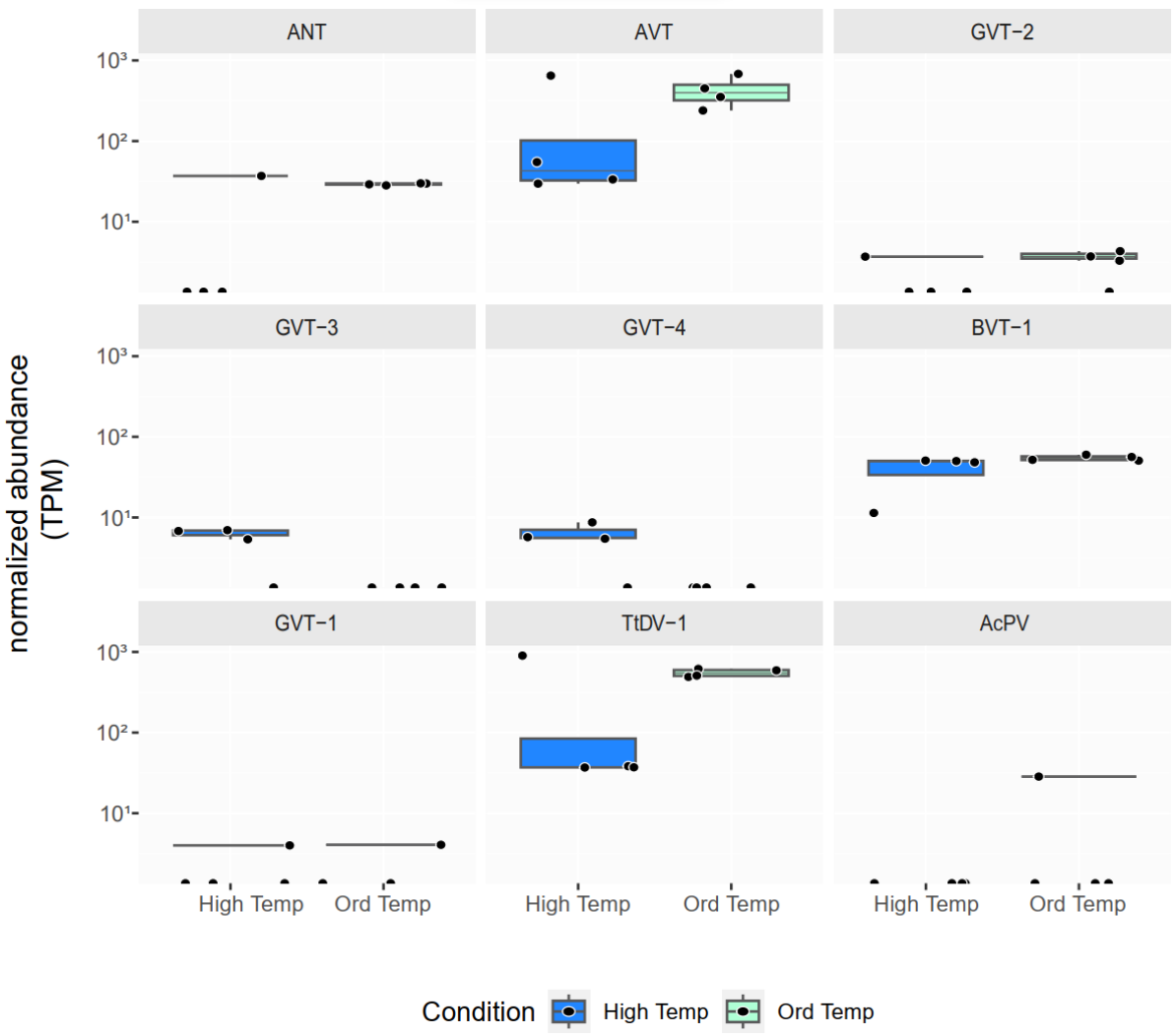

Figure S15: **Viral transcripts levels in libraries subjected to different temperature treatments**. The Y-axis represents the normalized abundance in TPM, while the X-axis categorizes the libraries into two treatment groups: High Temperature and Ordinary Temperature. The plot provides a visual comparison of TPM abundance, offering insights into the impact of temperature treatment on virus expression levels in the libraries.

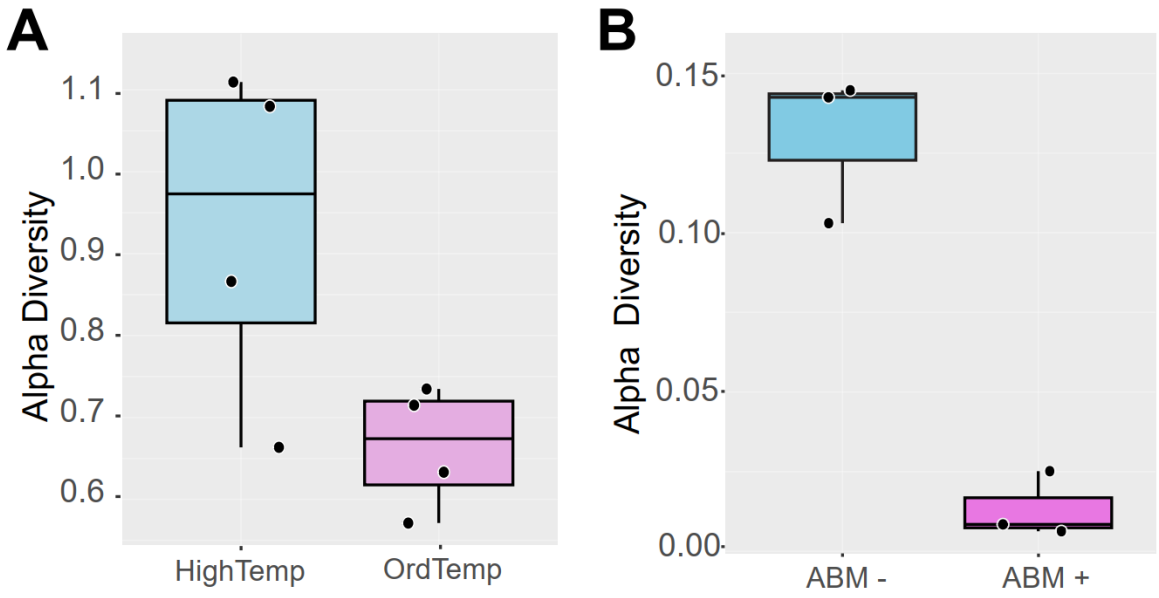

Figure S16: **Alpha diversity analysis of temperature and abamectin stress in *Tetranychus truncatus* virome**. Boxplot illustrating alpha diversity in libraries corresponding to temperature treatment (A) and abamectin treatment (B) conditions, including. The Y-axis represents alpha diversity, and the X-axis categorizes libraries based on the sample conditions.

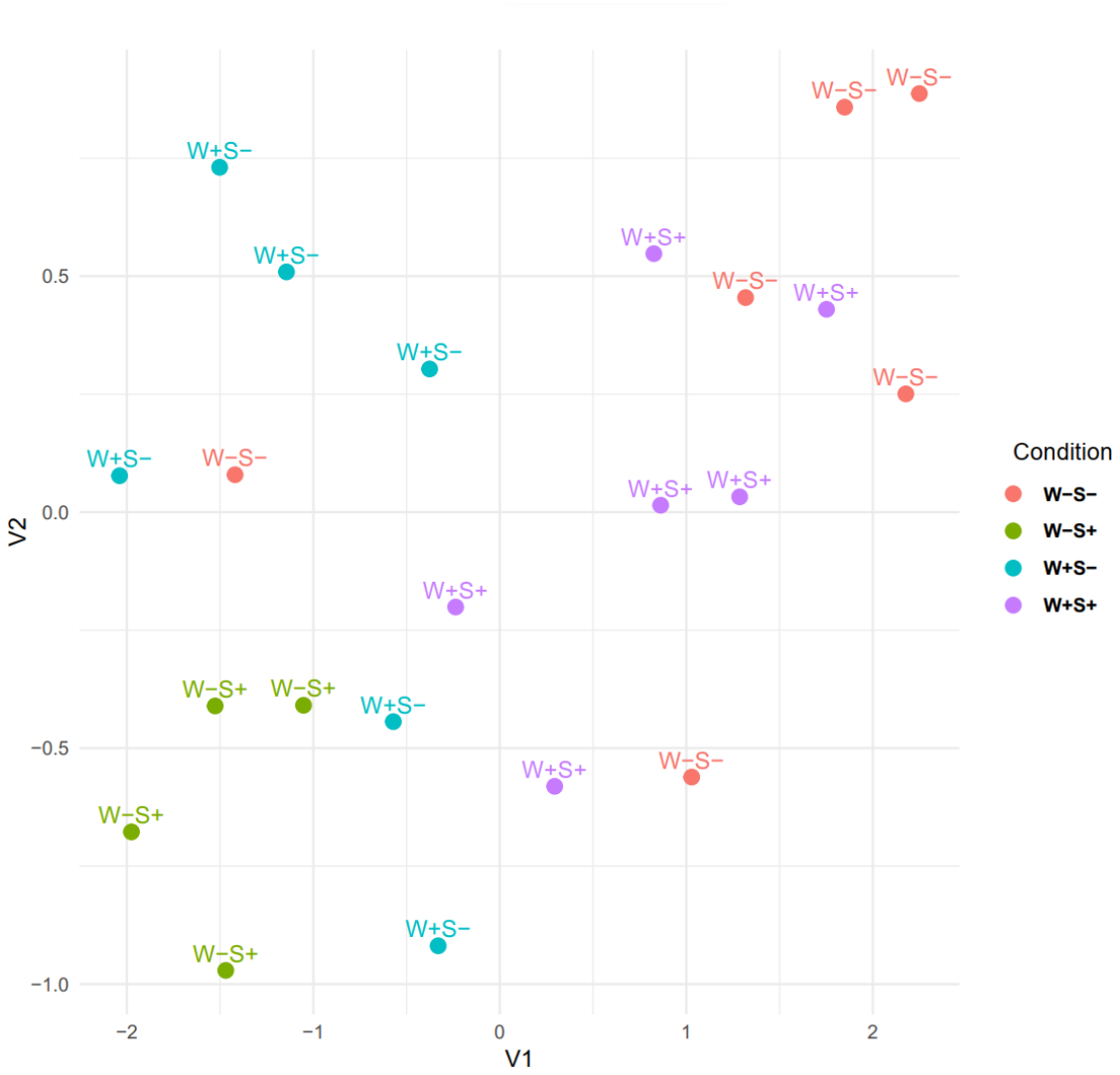

Figure S17. UMAP projections illustrate distinct transcriptional profiles of mites under different endosymbiont profiles. Samples derived from mites exclusively infected by *Wolbachia* are denoted in blue (W+S-), while exclusively infected with *Spiroplasma* in green (W-S+), coinfected by both Spiroplasma and Wolbachia in purple (W+S+), and uninfected in red (W-S-).

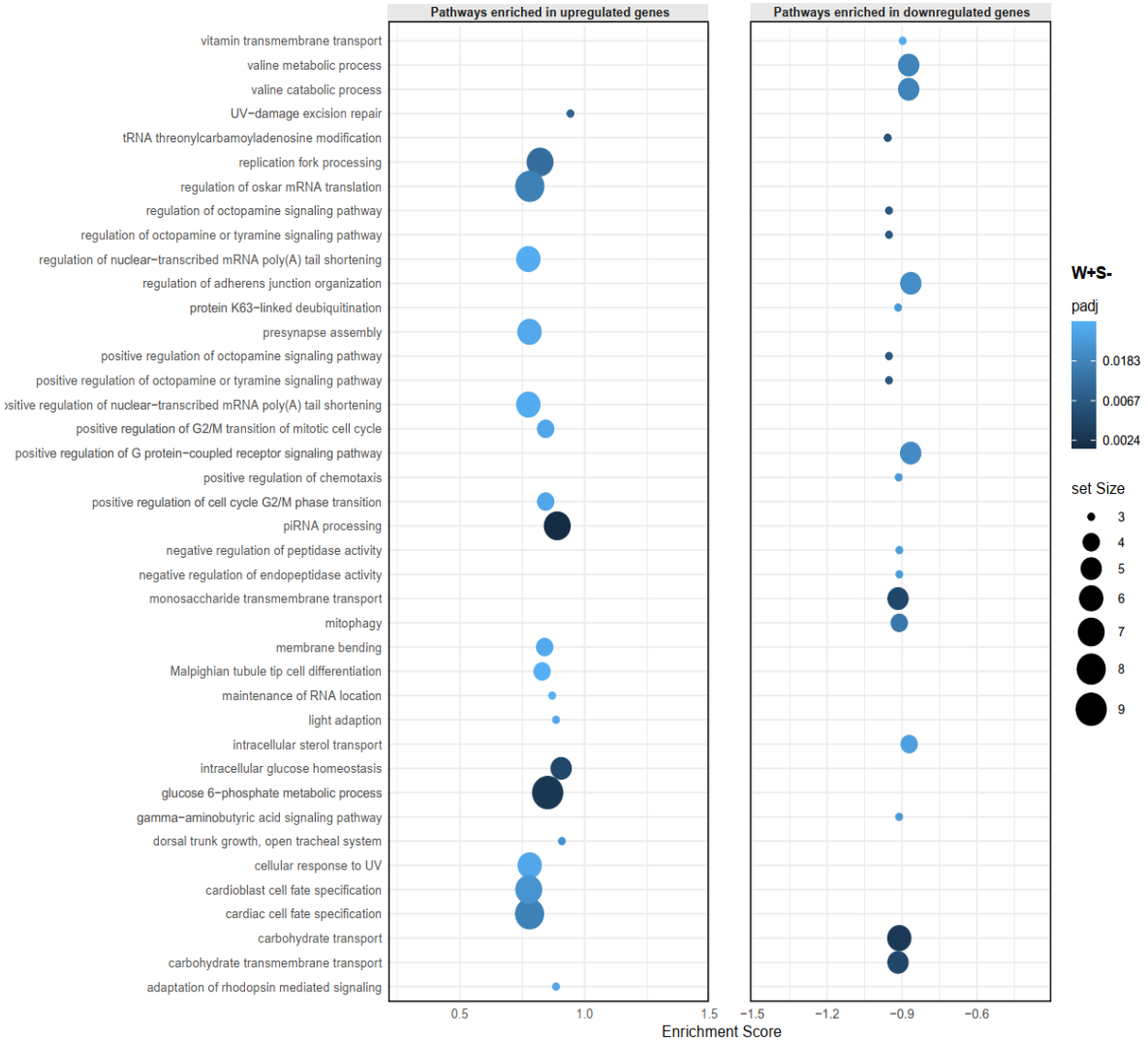

Figure S18. Pathways related to Enriched Gene Sets in *Tetranychus truncatus* exclusively infected by Wolbachia. The bubble plot illustrates pathways enriched in mites solely infected with *Wolbachia*, as determined by differential analysis in comparison to uninfected samples. Pathways are represented on the y-axis, while the Enrichment Score is depicted on the x-axis. The size of each bubble corresponds to the gene set size, and the color of the bubble scales with the adjusted *p*-value (padj).

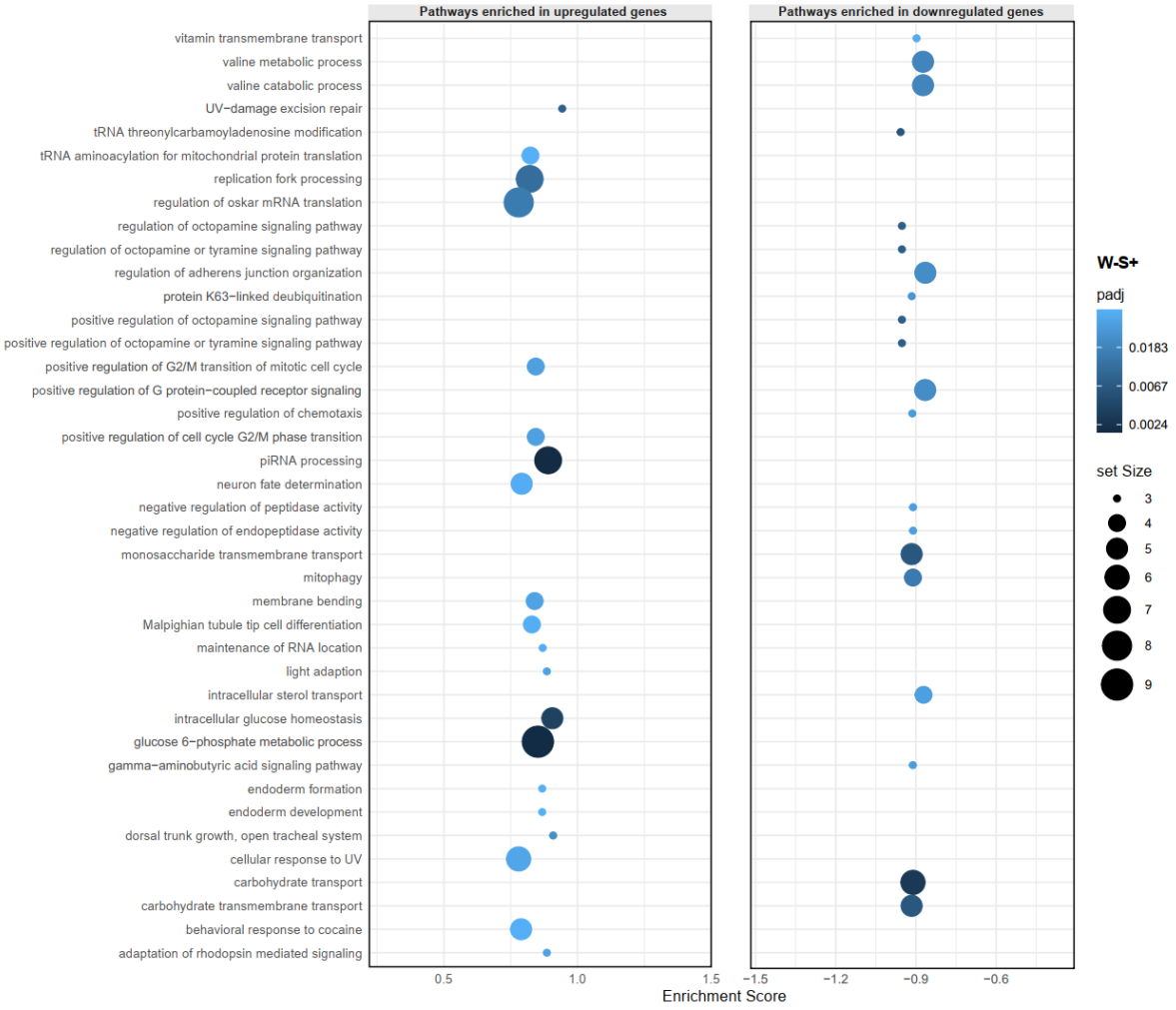

Figure S19. Pathways related to Enriched Gene Sets in *Tetranychus truncatus* exclusively infected by Spiroplasma. The bubble plot illustrates pathways enriched in mites solely infected with *Spiroplasma*, as determined by differential analysis in comparison to uninfected samples. Pathways are represented on the y-axis, while the Enrichment Score is depicted on the x-axis. The size of each bubble corresponds to the gene set size, and the color of the bubble scales with the adjusted *p*-value (padj).

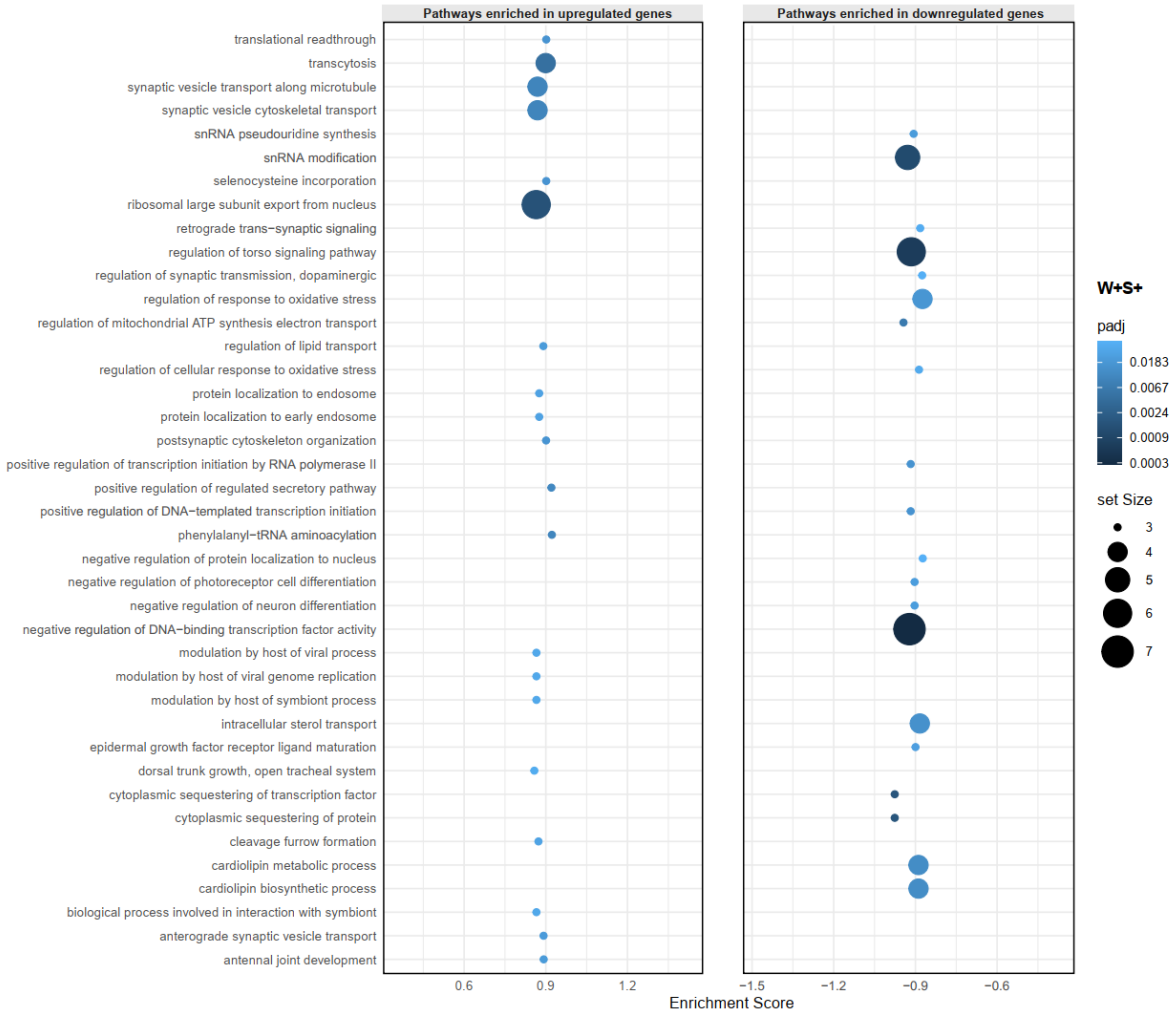

Figure S20. Pathways related to Enriched Gene Sets in *Tetranychus truncatus* coinfected by Wolbachia and Spiroplasma. The bubble plot illustrates pathways enriched in *Wolbachia* and *Spiroplasma* coinfected mites, as determined by differential analysis in comparison to uninfected samples. Pathways are represented on the y-axis, while the Enrichment Score is depicted on the x-axis. The size of each bubble corresponds to the gene set size, and the color of the bubble scales with the adjusted *p*-value (padj).